2023 IMEKO TC-4 International Conference on
Metrology for Archaeology and Cultural Heritage
Rome, Italy, October 19-21, 2023

Dimensional assessment in bioarchaeology applications: a preliminary study on quality controls in 3D printing of human skulls

Marta Cecchitelli[1], Giorgia Fiori[1], Gabriele Bocchetta[1], Federico Filippi[1], Fabio Leccese[2], Jan Galo[3], Salvatore Andrea Sciuto[1], Andrea Scorza[1]

[1] *Dep. of Industrial, Electronic and Mechanical Engineering, University of Roma TRE, Rome, Italy*
[2] *Dep. of Science, University of Roma TRE, Rome, Italy*
[3] *Clinical Engineering Service, IRCCS Children Hospital Bambino Gesù, Rome, Italy*

***Abstract* – In the last few years, three-dimensional (3D) printing has been used in archaeology and cultural heritage fields for different purposes. Among the different technologies of 3D printing, e.g., stereolithography or selective laser sintering, this study focuses on the quality assessment of printed models using fused deposition modeling technology. To simulate archaeological human remains, a cranial model assumed as a gold standard has been printed from computed tomography (CT) data of a human skull. Eight 3D printed (3DP) models have been reproduced and CT scanned with the same protocol in order to quantify their congruence with the gold standard through an objective measurement method based on image analysis. Preliminary results show an increasing percentage error as the degree of model detail increases, from 1% to 15%. The experimental results are discussed and commented also from a metrological point of view.**

I. INTRODUCTION

According to both scientific and technical literature, three-dimensional (3D) printing in archaeology and cultural heritage fields is used for different purposes, e.g., research, conservation, and access to museum exhibitions [1]. The 3D archives in museums (e.g., physical model, 3D printed model, simulated reconstruction) allow the preservation of features of finds and human remains while ensuring their display. In this way, the archaeological specimen, often already deteriorated, can be protected from swift and/or extreme changes in the condition of preservation. Furthermore, 3D printing has also been examined to show how it could be used for the inclusive valorization of cultural heritage [2]. In fact, it can support the fruition of those users affected by visual, cognitive, or sensory-perceptual disabilities. Another application in the archaeology field concerns the study of Egyptian mummies, now increasingly investigated by means of non-destructive techniques such as Computed Tomography (CT) [3,4]. Specimens can be physically reproduced by 3D printing using techniques developed in the biomedical field [5] to study anatomy from archaeological remains. In [6] has been shown the utility of the practice through a qualitative evaluation of the 3D printed models for ancient species identification. The 3D reconstruction is particularly useful when the original specimens are inaccessible or cannot be taken from the finding site for conservation reasons. For example, in 1993 a very well-preserved Neanderthal skeleton was discovered near the town of Altamura in Italy but in an unusual site with difficult access. The 3D reconstruction of the cranium using non-invasive acquisition techniques allowed the study of Neanderthal evolution through the observation of morphological traits without moving or handling the original specimens [7]. In addition, CT scanning and 3D printing allow the internal anatomical surfaces of bone remains to be analyzed and reproduced [8]. Despite the interest of Virtual Anthropology [9] in improving digital acquisition and faithful 3D reproduction of findings and human remains [10], there are no European regulatory requirements in terms of quality control for 3D printed models, unlike in the biomedical field, where the products of rapid prototyping for clinical purpose are recognized as medical devices [11,12]. The virtual reconstruction of archaeological specimens must be done in the most rigorous way to guarantee the truthfulness of the data being analyzed, and a standardized procedure is needed to minimize reproducibility errors [13]. In fact, to provide an accurate information to anthropologists for studying the human remains of Neolithic Age discovered in the Tyrolean Alps in 1991, in [14] the skull duplicated from the CT data by stereolithography was validated through a comparison of measurements obtained from the original CT images and from external physical measurements of the intact head of the mummy. The study here proposed is a first approach to quantitative dimensional analysis for quality control in bioarchaeology 3D printing from a metrological point of view. In particular, the assessment of dimensional compatibility was carried out between data acquired from a CT examination of a 3D printed (3DP)

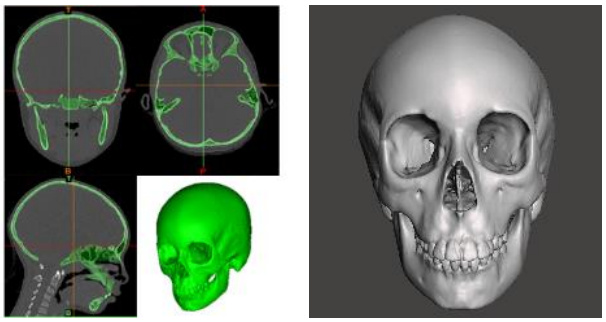

a *b*

Fig. 1. (a) 3D reconstruction of the skull from axial, coronal and sagittal views from CT exam; (b) gold standard to be printed and used as a simulated archaeological specimen.

model simulating archaeological human remains, i.e., a human skull, and CT data of eight replicas of the same obtained by digital segmentation and 3D printing using Fused Deposition Modeling (FDM) technology.

II. MATERIALS AND METHODS

In this study, a cranial model was 3D printed from CT data (Siemens Somatom Force® dual source tomograph [15]) acquired from the anonymous diagnostic exam of an 8-year-old patient to simulate an archaeological skull specimen. In this study, the anonymized data were used for scientific purposes, as usually done in the medical field [16,17]. The simulated specimen was used as a reference in the dimensional investigation and assumed as a gold standard. The DICOM dataset was imported into a dedicated medical 3D image-based engineering software: Mimics Materialise 25.0 (Leuven, Belgium). The digital segmentation was performed by a semi-automatic procedure. In order for the 3DP model to be for reference, the model mask, i.e., the 3D reconstruction of the skull from the CT images (Fig. 1a), was exported to Autodesk Meshmixer using the manual smoothing tool to remove any surface defects (Fig. 1b).

The actual skull size was reduced according to a scale of 1:0.75 to minimize material use and printing time while preserving details. Then, the segmented object was exported into Medical 3-matic 17.0 (Leuven, Belgium) and converted to a .stl file (Fig. 1b) taking care to achieve an optimized mesh minimizing the presence of artifacts (i.e., stitching, holes, overlaps, etc.) and suitable for the print file (.3mf). The G-code of the .3mf file, generated with UltiMaker Cura 5.2.2, was read by an UltiMaker S5 Pro Bundle printer [18] to reproduce the 3DP model assumed as the gold standard and named Skull0 (Fig. 2).

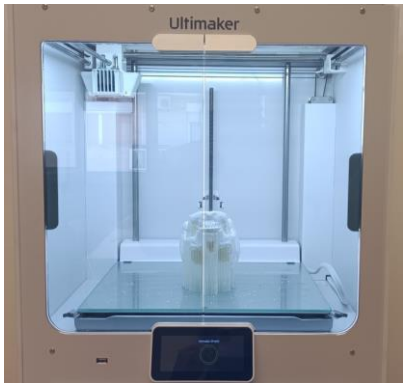

Fig. 2. Cranial model 3D printed with the UltiMaker S5 Pro Bundle assumed as the gold standard.

The printing parameters of the Skull0 were chosen the same as those used for the eight 3DP models (Table 1) except for the layer thickness, which was voluntarily chosen lower to ensure optimal surface quality according to the gold standard purpose.

All 3DP models in this study were printed in polylactic acid (PLA, extruder 1 in Table 1), besides being one of the most widely used materials in FDM 3D printing [19], it lends itself well to CT acquisition, responding to x-rays like bone without luminescence artifacts.

The support structure needed for FDM technology was set in polyvinyl alcohol (PVA, extruder 2 in Table 1) [20]: water-soluble material otherwise impossible to remove from a concave and complex geometry such as the skull. In addition, it ensures minimal interference between contact surfaces, a desirable condition for study purposes. For all 3DP models, the support structure was automatically generated for a 45° overhang angle.

Table 1. Main printing parameters.

Parameter	Extruder 1	Extruder 2
Material	PLA	PVA
Layer height: Skull0	0.1 mm	0.1 mm
Layer height: eight replicas	0.2 mm	0.2 mm
Infill density	10 %	-
Print temperature	205 °C	220 °C
Print speed	40 mm·s^{-1}	35 mm·s^{-1}

After the necessary cleaning and washing operations finished printing, the gold standard 3DP cranial model was scanned in CT. The high-resolution scanning protocol was performed according to the settings listed in Table 2.

The image data collected were segmented by thresholding in order to print replicas to be compared with the gold standard 3DP model. In particular, eight 3DP models were reproduced according to the same procedure adopted for the gold standard, except for manual smoothing operations to ensure the repeatability of the process. The software used, being dedicated to the biomedical field, reads CT images in HU (Hounsfield Units). In particular, the Hounsfield scale values are dimensionless units, universally used in CT scanning to quantify radiodensity [21], and linearly correlated with the

grayscale of images [22]. In brief, the model masks were obtained using a custom threshold set from -802 to 739 HU. The custom range used was chosen based on the x-ray response of the PLA. Then, the segmented objects were wrapped and smoothed for multiple automatic iterations with the same settings.

All segmented objects were loaded into Medical 3-matic 17.0 (Leuven, Belgium) to fix the mesh and to save the file as STL to source for printing. The STL files were imported into UltiMaker Cura 5.2.2 to be converted into G-code according to the parameters in Table 1. The eight 3DP cranial models were CT scanned with the same protocol used for the gold standard so that the dimensional comparison between the CT images of the gold standard and the ones of each replica could be carried out. Fig. 3 shows a picture of all the 3DP skulls considered in this study, i.e., Skull0 considered as the gold standard, and its eight replicas. All skulls were scanned according to the patient position indicated by the pediatric head CT protocol: they were housed in a dedicated stand and centered in the gantry according to a laser cruciform system (Fig. 4). To ensure the repeatability of the operation, the same experienced radiology technician was responsible for positioning the skulls.

The comparison was carried out between the mask obtained from the CT of the Skull0 and the mask obtained from the CT of each replica. An *ad hoc* objective method based on image analysis was implemented to verify the congruence of the model before and after the printing process, evaluating the quality of the results in terms of metrological compatibility of measurement results. Specifically, the analysis proposed was conducted in 2D selecting the slice of CT exam for which the largest outer diameter was automatically identified for each skull. The proposed method allowed the CT images of the replicas to be automatically segmented based on a threshold value expressed in grey levels of the images. These objective segmentations on the CT of the eight replicas resulted in the masks being dimensionally compared with the mask of Skull0.

Table 2. Main CT scanning protocol settings.

CT parameter	Setting
Step factor	0.55
Single collimation width	0.59 mm
Voltage peak	90 kV
Field of view	180 mm
Pixel size	0.35 × 0.35 mm^2
Slice increment	0.5 mm
Slice thickness	0.5 mm
Total number of slices	263

Fig. 3. Skull0 and its eight 3DP replicas.

III. RESULTS AND DISCUSSION

Identified by the proposed method the slice with the largest diameter for each skull, the comparison was conducted in terms of section area A, maximum longitudinal diameter D_{max}, and thicknesses identified at the latter (S_1 and S_2 in Fig. 5) in Table 3 and the difference (Δ) of the above quantities, expressed also as percentages (Table 4), detected between the masks of all replicas and the mask of the gold standard, respectively. In particular, the section area A has been evaluated as the total number

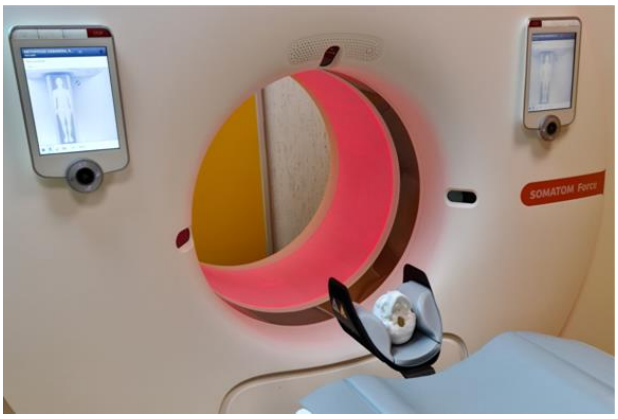

Fig. 4. 3DP cranial model CT scan in a dedicated stand.

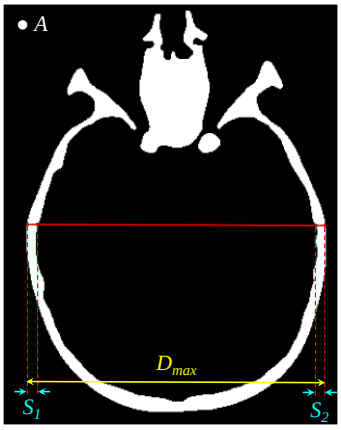

Fig. 5. Slice of the sample CT in which the measured quantities being compared are shown. A: area of skull section (white pixels); D_{max}: maximum longitudinal diameter; S_1 and S_2: skull thicknesses at D_{max}.

Table 3. Dimensional measurements on the model mask (mean ± SD).

3DP model	A (mm^2)	D_{max} (mm)	S_1 (mm)	S_2 (mm)
Skull0	2051 ± 1	101.1 ± 0.2	4.2 ± 0.2	3.9 ± 0.2
Skull1	2129 ± 27	101.4 ± 0.2	3.9 ± 0.2	4.4 ± 0.3
Skull2	1898 ± 10	101.1 ± 0.2	4.2 ± 0.2	4.5 ± 0.2
Skull3	2213 ± 2	101.3 ± 0.2	4.2 ± 0.2	4.5 ± 0.2
Skull4	2089 ± 29	101.1 ± 0.2	4.5 ± 0.2	3.9 ± 0.3
Skull5	2111 ± 2	99.8 ± 0.2	4.5 ± 0.2	3.9 ± 0.2
Skull6	1875 ± 2	101.1 ± 0.2	4.2 ± 0.2	4.5 ± 0.2
Skull7	1973 ± 8	101.7 ± 0.2	4.2 ± 0.2	4.0 ± 0.2
Skull8	2200 ± 40	101.7 ± 0.2	3.7 ± 0.2	4.2 ± 0.2

of white pixels of the selected slice and subsequently has been converted into mm^2 considering the pixel size in Table 2.

An uncertainty analysis was also conducted based on the main sources of error, these included the uncertainty on the pixel resolution of the CT images, while the uncertainty of the measurement image analysis was evaluated by a Monte Carlo simulation [23-26] with 10^4 iterations where the grey level threshold value for the mask of the replicas was made to vary randomly through a uniform distribution with ± 5% bounds. For a first estimation of the overall measurement uncertainty, shown in Table 3 and in Table 4, the above two uncertainty contributions were combined together by applying the uncertainty propagation law.

Table 3 shows the dimensional measurements for each skull at the section with the maximum longitudinal diameter. On the other hand, Table 4 shows the results of the comparison between each skull with Skull0 in percent (e.g., $\Delta_{i,0}$ expresses the relative differences between the i-th Skull and Skull0, where i = 1, 2, …, 8). The results are expressed in terms of mean ± standard deviation (SD).

The results obtained from dimensional measurements, except for area measurements discussed later, show that the largest contribution of uncertainty is due to pixel resolution. In fact, the SD of the measurement image analysis procedure is an order of magnitude smaller than that related to pixel size (Table 2).

The variation in the mean values of the parameters seems justified considering the variability of the printing process and the limitation of the whole technological process, starting from the slicing phase of the 3D mathematical model. In fact, the percentage error between the gold standard model and the replicas grows as the degree of detail of the object increases. The maximum discrepancy detected on the macroscopic parameters (D_{max}) is about 1% while for the two thicknesses an error higher than 15% is obtained.

In addition, the variability detected on the thicknesses S_1 and S_2 is consistent with uncertainty due to the printing - process: the printer nozzle has a diameter of 0.4 mm so,

Table 4. Differences of dimensional measurements between model masks (mean ± SD).

Δ	A (%)	D_{max} (%)	S_1 (%)	S_2 (%)
$\Delta_{1,0}$	3.80 ± 0.05	0.33 ± 0.01	5.0 ± 0.9	0.0 ± 0.2
$\Delta_{2,0}$	7.42 ± 0.04	0.03 ± 0.01	7.9 ± 1.4	9.1 ± 1.7
$\Delta_{3,0}$	7.93 ± 0.01	0.25 ± 0.01	8.3 ± 1.5	9.1 ± 1.7
$\Delta_{4,0}$	1.89 ± 0.03	0.15 ± 0.01	5.6 ± 1.2	17 ± 5
$\Delta_{5,0}$	2.93 ± 0.01	1.19 ± 0.01	8.3 ± 1.7	17 ± 3
$\Delta_{6,0}$	8.57 ± 0.01	0.08 ± 0.01	8.3 ± 1.5	9.1 ± 1.6
$\Delta_{7,0}$	3.76 ± 0.02	0.60 ± 0.01	4.6 ± 0.8	9.1 ± 2.2
$\Delta_{8,0}$	7.14 ± 0.14	0.66 ± 0.01	0.0 ± 0.2	4.7 ± 0.8

depending on the number of layers, there is a variability multiple of 0.4 mm on the mean value of thickness. The Δ values, expressed as the percentage difference of the compared thicknesses, are indicative of how many more or fewer layers the printer made in the section under consideration.

The spread of results obtained for the areas suggests that the section for which the maximum longitudinal diameter is detected may be not the same for Skull0 and its replica. The area outcomes are apart from each other in the slice range where anatomical geometry of the orbits and sinuses varies, causing variability in the cross-sectional area value, but the maximum diameter and thicknesses remain constant. This is likely due to the repeatability of the skull position during CT data acquisition.

IV. CONCLUSIONS

This study aims to provide a preliminary investigation of the quality of 3D printing for archaeological and cultural heritage applications. In particular, the application of 3D printing for the reproduction of finds and human remains should require a rigorous procedure to ensure accurate 3D replicas. Despite the widespread interest in the topic, further investigations are also required following a metrological approach for quality controls applied to 3D printed models. In this regard, the present study proposed an objective measurement method based on image processing to provide a dimensional comparison between an archaeological specimen and its replicas.

To simulate human remains, a cranial model 3D was reconstructed from CT data of a human skull and was printed using FDM technology. It was assumed as the gold standard and was scanned in CT with the high-resolution protocol. The dataset acquired was segmented to achieve eight 3DP replicas that were dimensionally compared with the gold standard model.

The study is focused on a preliminary approach to assessing the quality of the replicas. Therefore, since the overall differences in details are on the order of a few percentage points, it can be concluded that the replicas are suitable for museum exhibition installations. From the

measurement results the dispersion of the differences between replicas and the reference skull seems to depend on the variability of the printing process but also on the method uncertainty, due also to repeatability issues. Future developments will aim at investigating and quantifying the above two contributions. In this regard, further investigations should be performed on a higher number of dimensional measurements, e.g., the volume of the 3DP model by including all slices acquired from CT examination. Another issue to be investigated is concerned with the possible error related to the manual positioning of the 3DP models performed by the radiology technician. In addition, more samples could be subjected to dimensional verification by varying the geometry and printing parameters to find a discrepancy value to be considered as a maximum tolerance that ensures the quality of 3DP models. Finally, dimensional congruence could be investigated on 3DP models made by different printing technologies (e.g., stereolithography and selective laser sintering) to estimate the influence of technology on the results. In the future, the protocol here proposed could be improved and applied to the study of mummies and archaeological remains considered interesting from a historical point of view.

REFERENCES

[1] M.Neumüller, A.Reichinger, F.Rist, C.Kern, "3D printing for cultural heritage: preservation, accessibility, research and education", In: M.Ioannides, E.Quak (eds), "3D Research Challenges in Cultural Heritage", Lecture Notes in Computer Science, vol.8355, Springer, Berlin, Heidelberg, 2014, pp.119-134.

[2] E.Rossi, P.Barcarolo, "Use of digital modeling and 3D printing for the inclusive valorization of cultural heritage," Proc. of the International Conference on Applied Human Factors and Ergonomics (AHFE), 2018, pp. 257–269.

[3] L.M.McKnight, J.E.Adams, A.Chamberlain, S.D.Atherton-Woolham, R.Bibb, "Application of clinical imaging and 3D printing to the identification of anomalies in an ancient Egyptian animal mummy", J. Archaeol. Sci. Rep., vol.3, September 2015, pp.328-332.

[4] A.Du Plessis, R.Slabbert, L.C.Swanepoel, J.Els, G.J.Booysen, S.Ikram, I.Cornelius, "Three-dimensional model of an ancient Egyptian falcon mummy skeleton", Rapid Prototyp. J., vol.21, No.4, June 2015, pp.368-372.

[5] Z.Al-Dulimi, M.Wallis, D.K.Tan, M.Maniruzzaman, A.Nokhodchi, "3D printing technology as innovative solutions for biomedical applications", Drug. Discov. Today, vol.26, No.2, February 2021, pp.360-383.

[6] R.Bibb, L.McKnight, "Identification of bird taxa species in ancient Egyptian mummies: part 2, a qualitative evaluation of the utility of CT scanning and 3D printing", J. Archaeol. Sci. Rep., vol.46, No.103668, December 2022.

[7] A.Profico, C.Buzi, F.Di Vincenzo, M.Boggioni, A.Borsato, G.Boschian, D.Marchi, M.Micheli, J.M.Cecchi, M.Samadelli, M.A.Tafuri, J.L.Arsuaga, G.Manzi, "Virtual excavation and analysis of the early Neanderthal cranium from Altamura (Italy)", Commun. Biol., vol.6, No.316, March 2023.

[8] A.Profico, S.Schlager, V.Valoriani, C.Buzi, M.Melchionna, A.Veneziano, P.Raia, J.Moggi-Cecchi, G.Manzi, "Reproducing the internal and external anatomy of fossil bones: two new automatic digital tools", Am. J. Phys. Anthropol., vol.166, No.4, August 2018, pp.979-986.

[9] G.W.Weber, "Another link between archaeology and anthropology: virtual anthropology", Digit. Appl. Archaeol. Cult. Herit., vol.1, No.1, January 2014, pp.3-11.

[10] C.Buzi, I.Micarelli, A.Profico, J.Conti, R.Grassetti, W.Cristiano, F.Di Vincenzo, M.A.Tafuri, G.Manzi, "Measuring the shape: performance evaluation of a photogrammetry improvement applied to the Neanderthal skull Saccopastore 1", Acta IMEKO, vol.7, No.3, October 2018, pp.79-85.

[11] P.Nguyen, I.Stanislaus, C.McGahon, K.Pattabathula, S.Bryant, N.Pinto, J.Jenkins, C.Meinert, "Quality assurance in 3D-printing: a dimensional accuracy study of patient-specific 3D-printed vascular anatomical models", Front. Med. Technol., vol.5, No.1097850, February 2023.

[12] European Medicines Agency, "Human regulatory: medical devices", https://www.ema.europa.eu/en/human-regulatory/overview/medical-devices (accessed September 2023).

[13] L.Fregonese, N.Giordani, A.Adami, G.Bachinsky, L.Taffurelli, O.Rosignoli, J.Helder, "Physical and virtual reconstruction for an integrated archaeological model: 3D print and maquette", Int. Arch. Photogramm. Remote Sens. Spatial Inf. Sci., vol.XLII-2/W15, September 2019, pp.481-487.

[14] D.zur Nedden, R.Knapp, K.Wicke, W.Judmaier, W.A.Murphy Jr, H.Seidler, W.Platzer, "Skull of a 5,300-year-old mummy: reproduction and investigation with CT-guided stereolithography", Radiology, vol.193, No.1, October 1994, pp.269-272.

[15] Siemens Healthineers, "SOMATOM Force", https://www.siemens-healthineers.com/computed-tomography/dual-source-ct/somatom-force (accessed September 2023).

[16] H.Kikuchi, S.Ito, K.Ikegami, S.Shindo, "Diseases prediction from officially anonymized medical and healthcare big data," Proc. of 2022 IEEE International Conference on Big Data (Big Data), 2022.

[17] J.A.Onofrey, L.H.Staib, X.Papademetris, "Segmenting the brain surface from CT images with

artifacts using locally oriented appearance and dictionary learning", IEEE Trans. Med. Imaging, vol.38, No.2, February 2019, pp.596-607.

[18] Ultimaker, "Ultimaker S5 and Ultimaker S5 Pro Bundle: quick start guide", https://makerbot.my.salesforce.com/sfc/p/#j0000000HOnW/a/5b000004TWyi/KyTXfJ7VKhqF4cE6bXapRpSt98b1qrU7.beSCMA8m6U (accessed September 2023).

[19] E.H.Tümer, H.Y.Erbil, "Extrusion-based 3D printing applications of PLA composites: a review", Coatings, vol.11, No.4, March 2021.

[20] N.Y.Z.Ng, R.H.Abdul Haq, O.M.F.Marwah, F.H.Ho, S.Adzila, "Optimization of polyvinyl alcohol (PVA) support parameters for fused deposition modelling (FDM) by using design of experiments (DOE)", Mater. Today: Proc., vol.57, No.3, 2022, pp.1226-1234.

[21] A.Kalra, "Developing FE human models from medical images", In: K.-H.Yang (eds), "Basic Finite Element Method as Applied to Injury Biomechanics", Academic Press, 2018, pp.389-415.

[22] T.Razi, P.Emamverdizadeh, N.Nilavar, S.Razi, "Comparison of the Hounsfield unit in CT scan with the gray level in cone-beam CT", J. Dent. Res. Dent. Clin. Dent. Prospects, vol.13, No.3, Summer 2019, pp.177-182.

[23] JCGM 101:2008, "Evaluation of measurement data — Supplement 1 to the Guide to the expression of uncertainty in measurement — Propagation of distributions using a Monte Carlo method", 2008, https://www.bipm.org/documents/20126/2071204/JCGM_101_2008_E.pdf/325dcaad-c15a-407c-1105-8b7f322d651c (accessed September 2023).

[24] G.Fiori, F.Fuiano, A.Scorza, M.Schmid, S.Conforto, S.A.Sciuto, "ECG waveforms reconstruction based on equivalent time sampling," Proc. of 2020 IEEE International Symposium on Medical Measurements and Applications (MeMeA), 2020.

[25] F.Orsini, F.Fuiano, G.Fiori, A.Scorza, S.A.Sciuto, "Temperature influence on viscosity measurements in a rheometer prototype for medical applications: a case study," Proc. of 2019 IEEE International Symposium on Medical Measurements and Applications (MeMeA), 2019.

[26] G.Fiori, A.Pica, S.A.Sciuto, F.Marinozzi, F.Bini, A.Scorza, "A comparative study on a novel quality assessment protocol based on image analysis methods for Color Doppler ultrasound diagnostic systems", Sensors, vol.22, No.24, December 2022.